

# Zwicky Transient Facility and Globular Clusters: the *gr*-Band Period-Luminosity Relations for Mira Variables at Maximum Light and Their Applications to Local Galaxies

CHOW-CHOONG NGEOW,<sup>1</sup> JIA-YU OU,<sup>1</sup> ANUPAM BHARDWAJ,<sup>2</sup> JOSIAH PURDUM,<sup>3</sup> BEN RUSHOLME,<sup>4</sup> AND AVERY WOLD<sup>4</sup>

<sup>1</sup>*Graduate Institute of Astronomy, National Central University, 300 Jhongda Road, 32001 Jhongli, Taiwan*

<sup>2</sup>*INAF-Osservatorio astronomico di Capodimonte, Via Moiariello 16, 80131 Napoli, Italy*

<sup>3</sup>*Caltech Optical Observatories, California Institute of Technology, Pasadena, CA 91125, USA*

<sup>4</sup>*IPAC, California Institute of Technology, 1200 E. California Blvd, Pasadena, CA 91125, USA*

## ABSTRACT

Based on 14 Miras located in 7 globular clusters, we derived the first *gr*-band period-luminosity (PL) at maximum light for the large-amplitude Mira variables using the multi-year light-curve data collected from the Zwicky Transient Facility (ZTF). Since Miras are red variables, we applied a color-term correction to subsets of ZTF light curves, and found that such corrections do not have a large impact on period determinations. We applied our derived PL relations to the known extragalactic Miras in five local galaxies (Sextans, Leo I, Leo II, NGC6822 and IC1613), and determined their Mira-based distances. We demonstrated that our PL relations can be applied to short-period ( $\lesssim 300$  days) Miras, including those in the two most distant galaxies (NGC6822 and IC1613) in our sample even when only a portion of the light-curves around maximum light have detections. We have also shown that the long-period extragalactic Miras do not follow the PL relations extrapolated to longer periods. Hence, our derived PL relations are only applicable to the short-period Miras, which will be discovered in abundance in local galaxies within the era of Vera C. Rubin Observatory’s Legacy Survey of Space and Time.

## 1. INTRODUCTION

Mira variables (hereafter Miras, see [Mattei 1997](#), for a general review) are pulsating asymptotic giant branch (AGB) stars with periods longer than 100 days. Miras obey a period-luminosity (PL) relation, especially in the *K*-band or the bolometric magnitudes, because Miras are cool supergiants with radiation peaks in the near-infrared (NIR). Indeed, the majority of the PL relations derived, or calibrated (that is, calibrating the zero-point of the PL relation by fixing the slope), in the literature were in the *JHK*-band (mainly in the *K*-band) and/or being converted to bolometric magnitudes (for examples, see [Glass & Evans 1981](#); [Glass & Feast 1982](#); [Feast 1984](#); [Reid et al. 1988](#); [Feast et al. 1989](#); [Hughes & Wood 1990](#); [Groenewegen & Whitelock 1996](#); [Bedding & Zijlstra 1998](#); [Whitelock & Feast 2000](#); [Glass & Lloyd Evans 2003](#); [Rejkuba 2004](#); [Soszyński et al. 2005](#); [Feast et al. 2006](#); [Whitelock et al. 2008](#); [Matsunaga et al. 2009](#); [Tabur et al. 2010](#); [Ita & Matsunaga 2011](#); [Yuan et al.](#)

[2017](#), [2018](#); [Bhardwaj et al. 2019](#); [Grady et al. 2019](#); [Ita et al. 2021](#); [Andriantsaralaza et al. 2022](#); [Sun et al. 2022](#); [Sanders 2023](#)). Some of these studies also included the derivation of period-Wesenheit (PW) relations, or the addition of a color-term for a period-luminosity-color (PLC) relation. At wavelengths shorter than *J*-band, PL (and PLC) relations have been derived in various optical bands (including *I*-band and Gaia bands, [Ita & Matsunaga 2011](#); [Bhardwaj et al. 2019](#)) in addition to the NIR bands, as well as a single-band PL relation in photographic *m<sub>pg</sub>*-band ([van den Bergh 1984](#)) and *I*-band ([Ou & Ngeow 2022](#)). Beyond *K*-band, several works have also derived the mid-infrared PL relations ([Glass et al. 2009](#); [Matsunaga et al. 2009](#); [Riebel et al. 2010](#); [Ita & Matsunaga 2011](#); [Iwanek et al. 2021a](#)). Finally, based on a comprehensive multi-bands analysis for Miras in the Large Magellanic Cloud (LMC), [Iwanek et al. \(2021b\)](#) presented a set of synthetic PL relations in 42 bands ranged from  $0.37\mu\text{m}$  to  $25.5\mu\text{m}$ .

In light of the recent “Hubble Tension” (for general reviews, see [Verde et al. 2019](#); [Di Valentino et al. 2021](#); [Freedman 2021](#); [Shah et al. 2021](#); [Riess et al. 2022](#)), Miras offer an independent route to determine the  $H_0$  via the local distance scale ladder, with several advantages being mentioned in [Whitelock \(2013\)](#), [Macri \(2017\)](#),

Huang et al. (2018, 2020), and Sanders (2023). On the other hand, Miras are long-period variables implying the long-term monitoring of extragalactic Miras using space-based telescopes, such as the *James Webb Space Telescope (JWST)*, might not be trivial (in terms of scheduling, proposals competitions, etc). On the ground, the 10 years survey of the Vera C. Rubin Observatory’s Legacy Survey of Space and Time (LSST, Ivezić et al. 2019) will naturally provide such a long baseline suitable for Miras. Hence, in combination with its photometric depths, LSST is expected to detect numerous Miras in various types of nearby galaxies (Macri 2017). Indeed, Miras are included in the Roadmap for the LSST Transients and Variable Stars group (Hambleton et al. 2022) as one of the scientific targets/goals of the survey.

Our aim of this work is to derive the optical band PL relations at maximum light by using the homogeneous light curve data collected from the Zwicky Transient Facility (ZTF, Bellm et al. 2019a; Graham et al. 2019; Dekany et al. 2020) for Miras located in the globular clusters. Our work would be similar to the work of Menzies & Whitelock (1985) and Feast et al. (2002), but using the most up-to-date and homogeneous globular cluster distances as given in Baumgardt & Vasiliev (2021). We choose to derive the PL relations at maximum light because their dispersions were found to be smaller than the mean light counterparts (Kanbur et al. 1997; Bhardwaj et al. 2019; Ou & Ngeow 2022; Ou et al. 2023). Though not an optimal choice, the derived optical band PL relations will still be valuable in the era of LSST, because the six filters set employed by LSST (*ugrizy*) do not extend to the NIR. In this manuscript, Section 2 describes the sample of Miras in globular clusters and their extracted ZTF light curves. We then refined their periods in Section 3, followed by the derivation of PL relations at maximum light in Section 4. We applied our derived PL relations to a number of local group galaxies in Section 5. We concluded our work in Section 6 together with a brief discussion.

## 2. SAMPLE AND ZTF LIGHT CURVES

We started the compilation of Miras in globular clusters from the “Updated Catalog of Variable Stars in Globular Clusters” (Clement et al. 2001; Clement 2017, hereafter the Clement’s Catalog), and only selected variable stars of “M” type. V1 and V4 in Palomar 4 was marked as “SR” (semi-regular) in Clement’s Catalog, however they were reclassified as Mira in Grady et al. (2019). Hence, they were added to the compilation. After excluding known or suspected foreground objects, and V7 in Terzan 5 (because this Mira was found to be a non-member based on radial velocity measurement, see

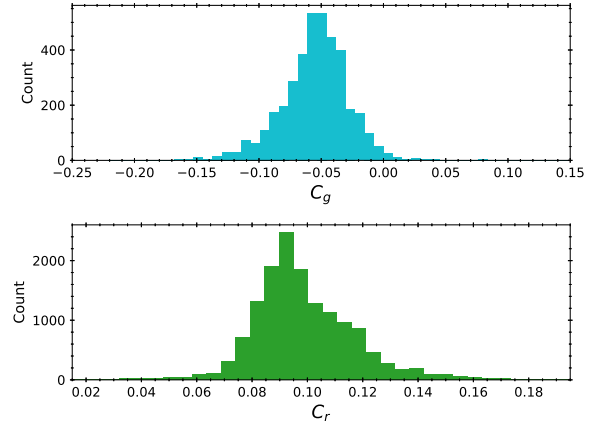


**Figure 1.** Distributions of color-coefficients,  $C_m$ , retrieved from the PSF catalogs for our sample of Miras. Upper and lower panels are for the  $g$ - and  $r$ -band, respectively.

Origlia et al. 2019), there were 23 Miras located in 10 globular clusters observable with ZTF ( $\delta_{J2000} > -30^\circ$ ).

For this initial sample of globular clusters Miras, we extracted the ZTF *gri*-band time-series photometric data from the PSF (point-spread function) catalogs, produced from a dedicated reduction pipeline (Masci et al. 2019), using a  $1''$  search radius. The PSF catalogs included those available from the ZTF Data Release (DR) 16 and the ZTF partner survey data<sup>1</sup> collected until 2023 March 31. We first visually inspected the ZTF light curves and remove those Miras with small number of data-points, or the data-points only sampling a small portion of the light curves within a single pulsating cycle. This step removed V4 in NGC 6553, V12 and V13 in NGC 6638, V5 and V6 in Terzan 5, V1 in Terzan 12. Three Miras in Terzan 5 either lack  $g$ -band or only contain very few  $g$ -band data points, and were subsequently removed because their single  $r$ -band ZTF light curves cannot be used to estimate colors (see next section). Hence, there are 14 Miras left in 7 globular clusters in the sample.

We have also excluded the  $i$ -band light curves, because there are 7 Miras in our sample that do not have any ZTF  $i$ -band data. For the remaining Miras, the numbers of data-points for the  $i$ -band light curves are in general smaller than other two filters,<sup>2</sup> and many of them only

<sup>1</sup> ZTF observations were divided into three parts, one of them being the partnership survey (for a further details, see Bellm et al. 2019a).

<sup>2</sup> After excluding light curves with null data, the averaged numbers of data points per light curves in the *gri*-band are 242.8, 821.3, and 193.6, respectively.

cover a portion of the light curve in a single pulsation cycle, preventing them to be analyzed further.

### 3. COLOR-CORRECTION ON LIGHT CURVES AND PERIODS REFINEMENT

As described in [Masci et al. \(2019\)](#), PSF photometry in ZTF catalogs were calibrated via  $m = m_{ZTF} + ZP_m + C_m(g - r)$ , where  $m = \{g, r\}$  is the calibrated magnitudes in the Pan-STARRS1 ([Chambers et al. 2016](#); [Magnier et al. 2020](#)) AB magnitude system, and  $m_{ZTF}$  represents the ZTF instrumental magnitudes. For non-varying sources, the  $(g - r)$  colors can be obtained from the Pan-STARRS1 catalog. For variable stars such as Miras, however, the time-dependent colors have to be known a priori. This is because the  $gr$ -band observations in ZTF are not simultaneous or near-simultaneous ([Bellm et al. 2019b](#)). Figure 1 shows the histograms for the color-coefficient,  $C_m$ , with medians of  $-0.053$  and  $0.096$  in the  $gr$ -band, respectively (the corresponding modes are  $-0.052$  and  $0.091$ ). Since Miras are very red variable stars, the calibrated light curves should include the  $C_m(g - r)$  color-terms.

Given the long period nature of Miras, the  $gr$ -band photometry taken within the same night, or within  $\sim 0.02P$  (where  $P$  is the pulsation period), can be treated as “near-simultaneous”. Hence, the time-dependent colors can be obtained via the following equation ([Ngeow 2022](#)):

$$(g - r) = \frac{(g_{ZTF} + ZP_g) - (r_{ZTF} + ZP_r)}{1 - C_g + C_r}. \quad (1)$$

We paired up the  $gr$ -band data-points that are closest in time, up to a threshold of  $\Delta MJD < 0.02P_n$  (where  $MJD$  is the modified Julian date), to construct the  $(g - r)$  colors. The period  $P_n$  was determined using the `LombScargleMultiband` module ([VanderPlas & Ivezić 2015](#)), available from the `astroML/gatspy` package,<sup>3</sup> on all of the  $gr$ -band light curves without the color-terms (hence the subscript  $n$  means no color-terms). Left panel of Figure 2 shows an example of the color-curve constructed using equation (1), while the right panels of Figure 2 present the  $gr$ -band light curves without (open circles) and with (filled circles) the inclusion of the color-terms. In general, the pairs of  $gr$ -band data-points separated by more than a night (green triangles in the left panel of Figure 2) closely resemble those taken within the same night, justifying our assumption that the colors can be constructed for Miras even if the data-points in two bands were taken from different nights.

<sup>3</sup> <https://github.com/astroML/gatspy>.

We have also determined the periods based on the subsets of  $gr$ -band light curve data-points that can be used to calculate the color-terms. When comparing the periods found in these subsets of light curves, the largest percentage difference is 0.1% between the light curves with and without the color-terms correction, suggesting the color-terms do not have a great impact on the determined periods (due to large amplitudes of Miras). The periods based on the subsets of light curves corrected for the color-terms are denoted as  $P_c$ . In general,  $P_c$  is also in good agreement with  $P_n$ , and the percentage differences between them are less than 1%. The only exception is NGC6642 V1, for which the full set of  $gr$ -band light curves, uncorrected for color-terms, give  $P_n = 131.1$  days. In contrast, the subset of color-corrected light curves returned a period of  $P_c = 204.6$  days. Figure 3 shows that the Lomb-Scargle (LS) periodograms for this Mira have similar peaks at both periods, suggesting aliasing is affecting its light curves. We adopted  $P_n = 131.1$  days for NGC6642 V1 because it is closer to the literature period of 127 days. We have also adopted  $P_n$  as the final periods for other Miras in our sample, because the total number of data-points for full set of  $gr$ -band light curves are  $\sim 2$  to  $\sim 5$  times more than the subsets of data-points for determining colors, and have a longer time-span (hence, reducing the impact of aliasing). Since  $P_n$  and  $P_c$  differ by less than 1%, errors on the adopted  $P_n$  are most likely at the 1%-level.

Finally, with the exception of NGC6638 V15, the percentage differences between our determined  $P_n$  and the literature periods ( $P_l$ ) varied from 0.04% to 6.28%. In all cases, light curves folded with  $P_n$  exhibit a smaller scatter, justifying our determined periods are robust. For NGC6638 V15, the literature period of  $P_l = 156$  days corresponds to the second highest peaks of the LS periodograms (see left panels of Figure 4). Nevertheless, our periods of  $P_n = 274.8$  days can fold the ZTF light curves better than the literature periods, as demonstrated in the middle panel of Figure 4. For completeness, the right panels of Figure 4 present the  $gr$ -band light curves and the  $(g - r)$  color curve for this Mira.

### 4. THE PL RELATIONS AT MAXIMUM LIGHT

Light curves of Miras are well-known to exhibit cycle-to-cycle variations (for some exemplar light curves, see [Iwanek et al. 2022](#)). Therefore, [Bhardwaj et al. \(2019\)](#) took the averages of the brightest 10% of the light curves as an estimate of magnitudes at maximum light,  $m_X$ . While [Ou & Ngeow \(2022\)](#) divided the light curves to different pulsating cycles, and took an averaged for  $m_X$  found in the pulsating cycles. We followed the approach

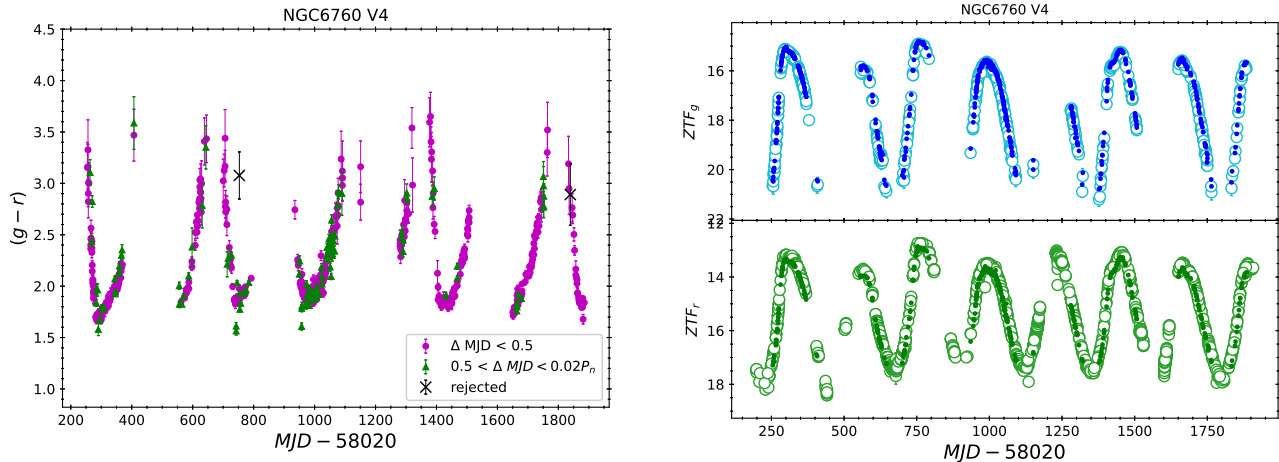


**Figure 2.** **Left Panel:** Color curve for one of the Miras in our sample constructed using equation (1). The “MJD” (modified Julian date) for the  $(g-r)$  data-points are at the mid-point of the  $gr$ -band MJDs. The magenta circles and green triangles are for the pairs of  $gr$ -band data-points taken in the same night ( $\Delta \text{MJD} < 0.5$  days) and taken on different nights up to  $0.02P_n$  days, respectively. Crosses are rejected data-points either with errors larger than 0.35 or with anomaly  $C_m$  values. **Right Panel:** The  $gr$ -band light curves for the same Miras as in the left panel. Open and filled circles in the  $gr$ -band light curves are those without and with the color-term corrections, respectively. Note that the color-term corrections did not apply to all  $gr$ -band data-points, only for those with the  $(g-r)$  counterparts. For clarity, error-bars are omitted in the right panels.

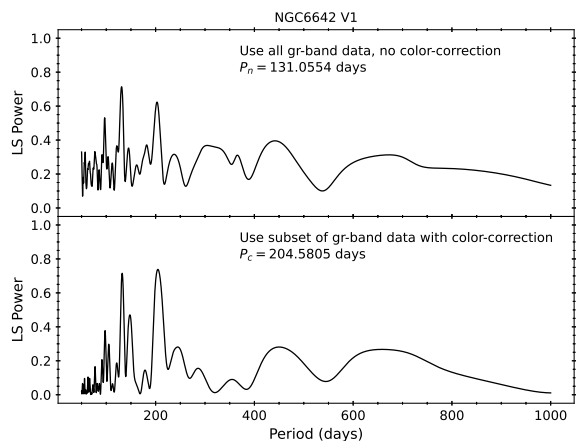


**Figure 3.** Comparison of the multi-band Lomb-Scargle (LS) periodograms for NGC6642 V1 based on the light curves with (upper panel) and without (lower panel) the corrections of color-terms.

laid out in [Ou & Ngeow \(2022\)](#) to determine the magnitudes at maximum light for our sample of globular cluster Miras. Briefly, we divided the ZTF  $gr$ -band light curves to a number of pulsation cycles according to the  $P_n$  determined in previous section. For  $i^{\text{th}}$  pulsation cycle, we fit a sinusoidal function to determine  $m_X^i$  if there are more than 10 data-points within the pulsation cycle and contain data-points around the maximum light (see [Figure 5](#) for two examples). In general, there are 2 to 10 pulsating cycles which satisfied our selection criteria for determining  $m_X^i$ , hence we took a mean as the final adopted  $m_X$  for our sample of Miras. The standard

deviations on  $m_X$ ,  $\sigma_X$ , were calculated based on small-number statistics ([Dean & Dixon 1951](#); [Keeping 1962](#), p. 202). The values of  $m_X$  and  $\sigma_X$ , together with periods determined in previous section, are summarized in [Table 1](#). In general,  $\sigma_X$  are in the order of  $\sim 0.5$  mag. This in turns reflect the fact that light curves for Miras are varying from cycle-to-cycle, resulting the magnitudes at maximum light fluctuate at the  $\sim 0.5$  mag level.<sup>4</sup>

By adopting the globular clusters distance  $D$  (in kpc) from [Baumgardt & Vasiliev \(2021\)](#) and the reddenings  $E$  from the [Bayerstar2019 3D reddening map](#) ([Green et al. 2019](#), hence the extinction corrections in the  $gr$ -band are  $3.518E$  and  $2.617E$ , respectively), we converted the magnitudes at maximum light listed in [Table 1](#) to absolute magnitudes ( $M_m^X$ ). The fitted linear PL relations for our sample of 14 globular clusters Miras, as shown in [Figure 6](#), are:

$$M_g^X = 4.118[\pm 0.649](\log P - 2.3) - 2.204[\pm 0.079], (2)$$

$$M_r^X = 3.262[\pm 0.562](\log P - 2.3) - 3.249[\pm 0.074], (3)$$

with a dispersion of 0.577 mag and 0.505 mag, respectively. [Iwanek et al. \(2021b\)](#) demonstrated that, based on synthetic PL relations at mean light, for wavelengths shorter than  $\sim 0.8\mu\text{m}$ , slopes of the PL relations are

<sup>4</sup> In general, amplitudes for shorter wavelengths light curves (such as  $gr$ -band) would be larger than the  $I$ -band or  $JHK$ -band light curves ([Iwanek et al. 2021b](#), their [Figure 2](#)). Hence, it is expected such fluctuations at maximum light would also be larger for shorter wavelengths light curves.

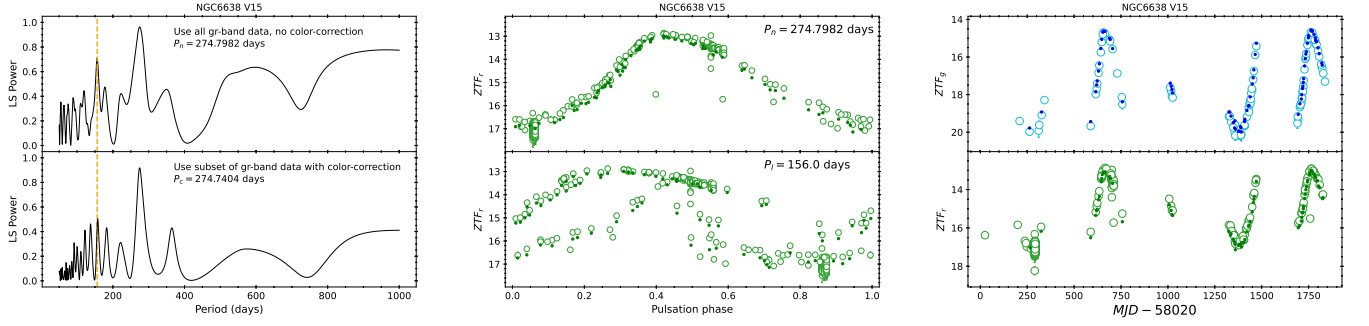


**Figure 4. Left Panel:** The multi-band LS periodograms based on the ZTF light curves, at which the highest peaks corresponding to  $P_n$  (upper panel) and  $P_c$  (lower panel). The vertical dashed line indicates the literature period of  $P_l = 156$  days. **Middle Panel:** Folded  $r$ -band light curves with our determined period  $P_n$  (upper panel) and literature period  $P_l$  (lower panel). The filled and open circles are data-points with and without color-terms correction, respectively. **Right Panel:** ZTF light curves and color curve for NGC6638 V15, where the symbols are same as the right panels of Figure 2.

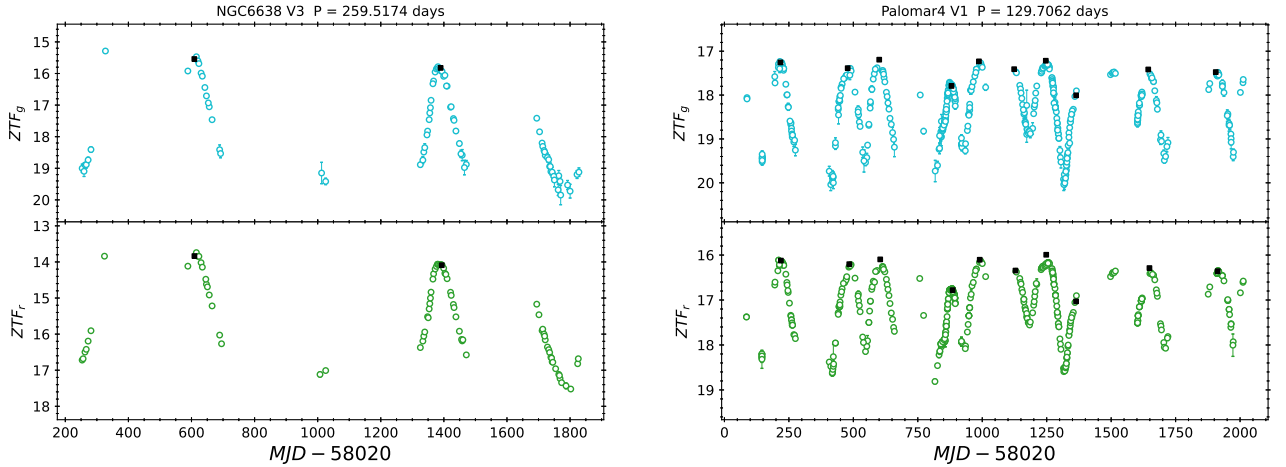


**Figure 5.** ZTF light curves for two Miras after corrected for the color-terms (open circles). The filled black squares are the determined magnitudes at maximum light, using the method described further in the text. Left panels show a Mira that only two  $m_X^i$  can be determined, while the right panels are for a Mira with a total of 10 determined  $m_X^i$ .

positive and decrease with wavelengths, at the same time the zero-points (or intercepts) of the PL relations and the PL dispersions are getting brighter and smaller, respectively. Our derived  $gr$ -band PL relations follow these trends, even though equation (2) and (3) were derived for magnitudes at maximum light. The positive PL slopes implying that the longer period Miras are fainter than their short period counterparts.

Miras can be classified into oxygen-rich (O-rich) and carbon-rich (C-rich) Miras. Using the determined periods  $P_n$  and  $JK$ -band photometry, adopted either from Sloan et al. (2010) or the Two Micron All Sky Survey (2MASS, Skrutskie et al. 2006), we classified the 14 globular clusters Miras as O-rich Miras based on the K-nearest neighbor (KNN) algorithm (as done in Ou et al. 2023). Furthermore, for samples of Miras that extended to  $\sim 1000$  days the PL relations were often fitted with either a segmented or a quadratic relation (for exam-

ples, see Ita & Matsunaga 2011; Yuan et al. 2017, 2018; Bhardwaj et al. 2019; Iwanek et al. 2021a; Ou & Ngeow 2022; Sanders 2023). In contrast, the longest period in our sample of Miras is  $\sim 300$  days (Palomar7 V3). Hence, strictly speaking the PL relations we derived in equation (2) & (3) are applicable to O-rich Miras with period less than 300 days.

## 5. APPLICATIONS TO LOCAL GALAXIES

Ou et al. (2023) demonstrated that ZTF could detect the peak brightness of known Miras in M33, which is located at a distance of 0.86 Mpc (or  $\mu = 24.67 \pm 0.07$  mag, de Grijs & Bono 2014). Therefore, we searched for local galaxies that are closer than M33, located within the visibility of ZTF, and contain known Miras detected from NIR observations. We identified five such galaxies: Sextans (Sakamoto et al. 2012), Leo I (Menzies et al. 2002, 2010), Leo II (Grady et al.

**Table 1.** Observed Properties of the Miras in Globular Clusters Studied in This Work.

Mira	$P_l^a$ (days)	$P_n$ (days)	$P_c$ (days)	$N_g$	$N_r$	$N_c^b$	$N_X^b$	$g_X$	$\sigma_g$	$r_X$	$\sigma_r$	$D$ (kpc) <sup>c</sup>	$E^d$
NGC6356 V1	230.6	226.7	227.0	83	423	61	3	15.377	0.353	13.941	0.397	$15.66 \pm 0.92$	$0.366 \pm 0.002$
NGC6356 V3	220.0	220.4	220.4	229	732	100	3	14.778	0.397	13.426	0.487	$15.66 \pm 0.92$	$0.366 \pm 0.002$
NGC6356 V5	219.8	220.6	220.0	256	734	100	4	15.033	0.298	13.650	0.308	$15.66 \pm 0.92$	$0.412 \pm 0.002$
NGC6638 V3	260.0	259.5	260.8	105	584	79	2	15.682	0.250	13.963	0.225	$9.78 \pm 0.34$	$0.410 \pm 0.003$
NGC6638 V15	156.0	274.8	274.7	93	608	73	2	14.512	0.197	13.052	0.065	$9.78 \pm 0.34$	$0.376 \pm 0.002$
NGC6638 V63	213.0	214.2	215.8	122	615	86	3	14.232	0.299	12.827	0.450	$9.78 \pm 0.34$	$0.472 \pm 0.004$
NGC6642 V1	127.0	131.1	204.6	125	621	79	2	14.033	0.217	12.379	0.194	$8.05 \pm 0.20$	$0.484 \pm 0.002$
NGC6712 V7	193.0	190.2	190.4	265	1093	198	4	12.768	0.293	11.308	0.421	$7.38 \pm 0.24$	$0.400 \pm 0.003$
NGC6760 V3	251.0	248.4	248.7	422	2152	411	5	15.193	0.261	13.407	0.273	$8.41 \pm 0.43$	$0.772 \pm 0.004$
NGC6760 V4	226.0	225.9	226.0	642	2770	605	7	15.344	0.404	13.460	0.433	$8.41 \pm 0.43$	$0.772 \pm 0.004$
Palomar4 V1	130.0	129.7	129.7	575	826	451	10	17.438	0.264	16.332	0.337	$101.39 \pm 2.57$	$0.124 \pm 0.009$
Palomar4 V2	150.0	150.7	150.3	557	827	444	8	17.111	0.228	15.950	0.288	$101.39 \pm 2.57$	$0.124 \pm 0.009$
Palomar7 V1	222.0	236.4	236.6	230	688	179	3	16.180	0.374	14.035	0.348	$4.55 \pm 0.25$	$1.142 \pm 0.002$
Palomar7 V3	300.0	297.9	295.2	174	687	147	4	16.006	0.499	13.814	0.387	$4.55 \pm 0.25$	$1.146 \pm 0.004$

<sup>a</sup> Published period as given in the literature.

<sup>b</sup>  $N_c$  is the number of data-points for constructing the color curves (i.e., pairs of  $gr$ -band photometry separated within  $0.02P_n$  days);  $N_X$  is the number of measured magnitudes at maximum light (see text for more details).

<sup>c</sup> Distance of the host globular clusters adopted from [Baumgardt & Vasiliev \(2021\)](#).

<sup>d</sup> Reddening value returned from the Bayerstar2019 3D reddening map ([Green et al. 2019](#)) at the location of the Miras in the globular clusters.

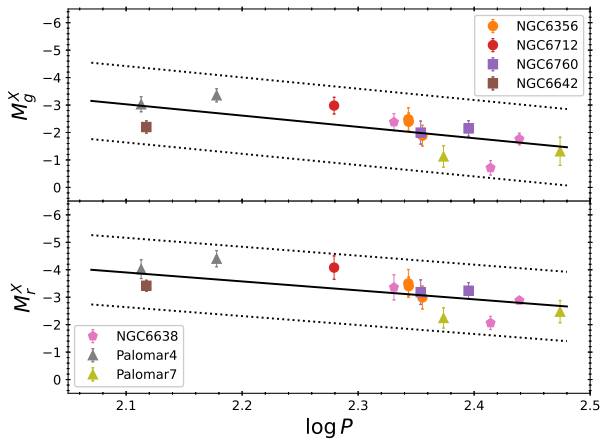


**Figure 6.** The extinction-corrected PL relations in the  $gr$ -band for the 14 globular clusters Miras as listed in Table 1. The solid lines are the fitted PL relations, while the dotted lines represent the  $\pm 2.5\sigma$  boundaries. Note that these PL relations are fitted for magnitudes at maximum light, and not the mean lights.

2019), NGC6822 ([Whitelock et al. 2013](#)), and IC1613 ([Menzies et al. 2015](#)). Literature distance modulus  $\mu$  for Leo I, Leo II, and Sextans were adopted from [Drlica-Wagner et al. \(2020\)](#) as  $\mu_{\text{Sextans}} = 19.7$  mag,  $\mu_{\text{Leo I}} = 22.0$  mag, and  $\mu_{\text{Leo II}} = 21.8$  mag, respectively. In case of NGC6822 and IC1613, [Parada et al. \(2023\)](#) summarized recent distance measurements to these two galaxies. We adopted the mid-point of the maximum and minimum  $\mu$  listed in their Table 10 and 11, as

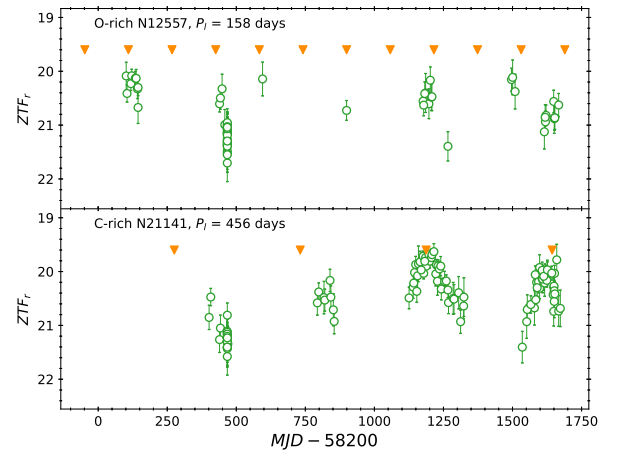


**Figure 7.** Examples of  $r$ -band ZTF light curves for two Miras in NGC6822. The orange triangles marked the expected epochs of maximum light (based on the literature period), and the brightest observed data-points tend to be found near these orange triangles.

$\mu_{\text{NGC6822}} = 23.4$  mag and  $\mu_{\text{IC1613}} = 24.3$  mag (this value is also same as the recommended value given in [de Grijs & Bono 2014](#)), respectively.

Three extragalactic Miras (L2077 in Leo I, N21029 in NGC6822, and SDSSJ101525.93-020431.8 in Sextans) are known to exhibit a (periodic) long-term trend, and hence they were excluded from the sample. For the rest of the Miras in these five local galaxies, we extracted their light curves from the ZTF DR16 and the partner survey data (in the same way as the globular clusters

**Table 2.** Observed Properties and the Derived Distance Modulus for Miras in the Local Galaxies.

Mira	$P_l$ (days)	$P_n$ (days)	$N_g$	$N_r$	$N_c$	$N_X$	$g_X$	$\sigma_g$	$r_X$	$\sigma_r$	$E^a$	$\mu_g$	$\mu_r$
Short-period O-rich Miras													
Sextans SDSSJ101234.29-013440.8	122	120.4	369	494	285	6	16.929	0.115	15.887	0.073	$0.072 \pm 0.005$	$19.78 \pm 0.67$	$19.66 \pm 0.61$
LeoII CRTSJ111320.6+221116	184	181.7	199	454	154	6	19.564	0.092	18.058	0.064	$0.208 \pm 0.002$	$21.20 \pm 0.59$	$20.90 \pm 0.53$
LeoI L8026	180	198.9	88	542	78	2	20.285	0.050	18.571	0.093	$0.248 \pm 0.014$	$21.62 \pm 0.58$	$21.18 \pm 0.53$
NGC6822 N12557	158	...	...	61	...	...	...	...	20.227	0.032	$0.316 \pm 0.002$	...	$23.12 \pm 0.55$
NGC6822 N12790	182	...	...	42	...	...	...	...	20.233	0.111	$0.258 \pm 0.007$	...	$23.08 \pm 0.54$
NGC6822 N20540	223	...	...	165	...	...	...	...	20.200	0.043	$0.276 \pm 0.007$	...	$22.72 \pm 0.53$
IC1613 G4237	178	...	...	29	...	...	...	...	20.991	0.083	$0.010 \pm 0.003$	...	$24.38 \pm 0.54$
Long-period O-rich Miras													
NGC6822 N20331	314	...	39	149	...	...	19.740	0.076	18.634	0.070	$0.262 \pm 0.002$	...	...
NGC6822 N10184	370	...	...	119	...	...	...	...	19.524	0.162	$0.258 \pm 0.007$	...	...
NGC6822 N30133	401	...	...	28	...	...	...	...	19.243	0.021	$0.292 \pm 0.006$	...	...
NGC6822 N20134	402	...	4	88	...	...	...	...	19.618	0.065	$0.270 \pm 0.004$	...	...
NGC6822 N40139	545	...	44	127	...	...	20.161	0.181	18.497	0.089	$0.276 \pm 0.007$	...	...
NGC6822 N10198	602	...	30	244	...	...	20.400	0.069	19.462	0.018	$0.206 \pm 0.004$	...	...
NGC6822 N30292	637	...	7	203	...	...	...	...	19.470	0.161	$0.302 \pm 0.004$	...	...
NGC6822 N10091	638	...	3	39	...	...	...	...	18.918	0.028	$0.206 \pm 0.004$	...	...
NGC6822 N20004	854	693.6	180	396	168	2	18.033	0.327	16.351	0.363	$0.276 \pm 0.007$	...	...
IC1613 G1016	464	...	141	397	...	...	20.021	0.092	18.825	0.088	$0.000 \pm 0.000$	...	...
IC1613 G1017	580	...	83	191	...	...	19.605	0.106	18.508	0.100	$0.000 \pm 0.000$	...	...
IC1613 G2035	530	...	65	212	...	...	19.832	0.081	18.730	0.059	$0.000 \pm 0.000$	...	...
IC1613 G3011	550	...	42	137	...	...	19.606	0.041	18.581	0.057	$0.000 \pm 0.000$	...	...
C-rich Miras													
LeoI L1019	158	160.5	54	470	41	1	20.634	...	18.981	...	$0.248 \pm 0.014$	$22.36 \pm 0.60$	$21.89 \pm 0.54$
LeoI L1077	336	...	...	55	...	...	...	...	20.130	0.217	$0.178 \pm 0.007$	...	$22.17 \pm 0.62$
NGC6822 N10817	214	...	100	327	...	...	20.238	0.089	19.831	0.054	$0.280 \pm 0.005$	$21.33 \pm 0.58$	$22.25 \pm 0.53$
NGC6822 N40590	223	...	...	78	...	...	...	...	20.946	0.032	$0.206 \pm 0.004$	...	$23.50 \pm 0.52$
NGC6822 N12751	231	...	...	140	...	...	...	...	20.389	0.098	$0.258 \pm 0.007$	...	$22.76 \pm 0.53$
NGC6822 N11032	239	...	...	104	...	...	...	...	20.703	0.046	$0.316 \pm 0.002$	...	$22.87 \pm 0.53$
NGC6822 N20578	246	...	...	61	...	...	...	...	20.437	0.084	$0.236 \pm 0.002$	...	$22.77 \pm 0.54$
NGC6822 N20542	255	...	...	190	...	...	...	...	20.251	0.034	$0.276 \pm 0.007$	...	$22.43 \pm 0.53$
NGC6822 N30430	269	...	...	59	...	...	...	...	20.405	0.080	$0.292 \pm 0.006$	...	$22.47 \pm 0.55$
NGC6822 N12208	278	...	12	92	...	...	...	...	19.879	0.022	$0.280 \pm 0.005$	...	$21.93 \pm 0.55$
NGC6822 N30583	302	...	1	76	...	...	...	...	20.954	0.074	$0.254 \pm 0.002$	...	$22.95 \pm 0.56$
NGC6822 N40114	312	...	4	35	...	...	...	...	20.835	0.062	$0.302 \pm 0.004$	...	$22.66 \pm 0.57$
NGC6822 N11059	319	...	1	25	...	...	...	...	20.728	0.259	$0.258 \pm 0.007$	...	$22.64 \pm 0.63$
NGC6822 N20657	343	...	...	25	...	...	...	...	20.705	0.183	$0.262 \pm 0.002$	...	$22.50 \pm 0.61$
NGC6822 N40520	432	...	3	34	...	...	...	...	20.791	0.152	$0.206 \pm 0.004$	...	$22.41 \pm 0.67$
NGC6822 N10753	432	...	...	115	...	...	...	...	20.700	0.109	$0.280 \pm 0.005$	...	$22.12 \pm 0.66$
NGC6822 N21141	456	...	...	107	...	...	...	...	19.894	0.068	$0.236 \pm 0.002$	...	$21.36 \pm 0.67$
IC1613 G4251	263	...	...	34	...	...	...	...	21.050	0.068	$0.000 \pm 0.000$	...	$23.91 \pm 0.54$
IC1613 G3083	280	...	...	42	...	...	...	...	20.689	0.229	$0.000 \pm 0.000$	...	$23.46 \pm 0.59$
IC1613 G3144	364	...	...	31	...	...	...	...	20.671	0.175	$0.000 \pm 0.000$	...	$23.07 \pm 0.63$
IC1613 G4183	410	...	...	17	...	...	...	...	21.040	0.066	$0.000 \pm 0.000$	...	$23.27 \pm 0.64$

<sup>a</sup> Reddening value returned from the Bayerstar2019 3D reddening map (Green et al. 2019).

Miras, see Section 2). Nevertheless, about half of them either do not have ZTF light curve data or only contain very few data points in the  $g$ - and/or  $r$ -band (mostly for the two distant galaxies NGC6822 and IC1613). For the remaining Miras, we re-classified them into the O-rich and C-rich Miras based on their  $JK$ -band photometry published in the aforementioned publications and the same KNN algorithms applied on the globular clusters Miras.

Based on the quality and the number of data-points on the ZTF light curves, we analyzed these Miras using two approaches. In case there are enough number of data-points in the  $gr$ -band ZTF light curves, we followed the same procedures as the globular clusters Miras to determine their  $P_n$ ,  $m_X$  and  $\sigma_X$ . This approach was only applied to five Miras. Otherwise we adopted the literature periods and only determine the  $m_X$  and  $\sigma_X$ , mostly in the  $r$ -band, by taking the means of the brightest 10% data-points (that is, following the approach as

outlined in [Bhardwaj et al. 2019](#)). This is because for Miras in the distant galaxies, it is possible that only the portion of the light curves around maximum light could be detected by ZTF (note that the limiting magnitude for ZTF is  $r \sim 20.6$  mag, [Bellm et al. 2019a](#)), as illustrated in [Figure 7](#). We then applied the color-term corrections on these brightest 10% data-points by adding  $C_m(g_X - r_X)$  to their calibrated magnitudes, where  $C_m$  were extracted from the ZTF PSF catalogs for individual data-points. Assuming the  $(g - r)$  colors at maximum light can be approximated with  $(g_X - r_X)$ , and fitting the globular clusters Miras in [Table 1](#) yields:

$$(g_X - r_X) = 0.910[\pm 1.763](\log P - 2.3) + 1.522[\pm 0.216], \quad (4)$$

with a dispersion of 0.299 mag.<sup>5</sup> The measured  $P_n$  (if applicable),  $m_X$ ,  $\sigma_X$ , and other relevant information are summarized in [Table 2](#).

### 5.1. Short-Period O-Rich Miras

There are seven O-rich Miras with period shorter than 300 days (i.e. short period) detected in all five galaxies. [Figure 8](#) presents three Miras which have ZTF light curves in both  $gr$ -band. We calculated the distance moduli for these seven Miras using our derived PL relations (presented in [Section 4](#)), they are listed in the last two columns of [Table 2](#). The derived distance moduli for Sextans SDSSJ101234.29-013440.8, NGC6822 N12557 and N12790, as well as IC1613 G4237 are in good agreement with the literature values. The Mira CRTSJ111320.6+221116 in Leo II has a smaller distance modulus, especially in the  $r$ -band, when compared to the literature  $\mu_{\text{Leo II}} = 21.8$  mag. [Grady et al. \(2019\)](#) also found a shorter distance ( $193 \pm 15$  kpc) for this Mira, using a totally independent dataset and PL relation, with respect to Leo II ( $233 \pm 14$  kpc). Therefore, our result is consistent with the finding of [Grady et al. \(2019\)](#). The  $r$ -band distance moduli for Leo I L8026 and NGC6822 N20540 were also smaller, nevertheless they are still fall within  $\sim \pm 1.5\sigma$  from the literature values.

By adopting the literature  $\mu$ , the absolute magnitudes of these seven short-period extragalactic O-rich Miras were compared to the globular clusters Miras in the left panels of [Figure 9](#). With the exception of Leo I L8026, all other short-period O-rich Miras are consistent with globular cluster Miras and located within the  $\pm 2.5\sigma$  boundaries of the  $r$ -band PL relation.

<sup>5</sup> The extinction-corrected version of this relation is:  $(g_X - r_X)_0 = 0.110[\pm 0.846](\log P - 2.3) + 1.124[\pm 0.107]$ , with a dispersion of 0.103 mag.

### 5.2. Long-Period O-Rich Miras

NGC6822 and IC1613 are the only two galaxies in our sample containing O-rich Miras with period longer than 300 days. The long-period O-rich Miras in NGC6822 and IC1613, as shown in [Whitelock et al. \(2013\)](#) and [Menzies et al. \(2015\)](#), respectively, were known to be over-luminous in the  $K$ -band and the bolometric magnitude. These over-luminous Miras were presumably undergoing hot bottom burning (HBB) phase (for examples, see [Whitelock et al. 2003](#); [Ita & Matsunaga 2011](#)). For the long-period O-rich Miras listed in [Table 2](#), their  $gr$ -band absolute magnitudes were also much brighter than the magnitudes predicted from extrapolating the PL relations to a longer period, as demonstrated in the left panels of [Figure 9](#). Interestingly, after excluding the longest-period Mira, these long-period O-rich Miras seems to have a near constant or mildly period-dependent  $gr$ -band absolute magnitudes at maximum light. Since the ZTF light curves are incomplete for these long-period Miras, and color-term corrections using equation (4) might not be valid for them, the existence of such a near constant absolute magnitude is not conclusive. The much deeper and 10 years light curves data collected from LSST can be used to investigate these long-period Miras further, because both galaxies are located within the footprint of LSST.

### 5.3. C-Rich Miras

In the era of synoptic sky surveys such as LSST, newly discovered extragalactic Miras may lack NIR photometry or spectroscopic observations to be classified to O-rich or C-rich. Hence, the C-rich Miras in Leo I, NGC6822 and IC1613 provide an opportunity to test the distance measurement if a genuine C-rich Miras discovered from optical surveys was mis-identified as an O-rich Mira. However, the majority of them only contain incomplete  $r$ -band light curves, and suffer the same problems as the long-period O-rich Miras (see the discussion in sub-section 5.2), the derived distance moduli for these C-rich Miras, listed in the last two columns of [Table 2](#) using equation (2) and (3), should be treated with caution.

The  $gr$ -band distance moduli of the two C-rich Miras in Leo I are in good agreement with the literature  $\mu$  of  $\mu_{\text{Leo I}} = 22.0$  mag. In the case of C-rich Miras in both NGC6822 and IC1613, except for a few short-period Miras, the derived distance moduli were smaller than the literature values. In other words, they seem to be slightly over-luminous at a given period, as shown in the right panels of [Figure 9](#). The long-period C-rich Miras are also tend to be over-luminous, similar to the cases of long-period O-rich Miras. The right panels of



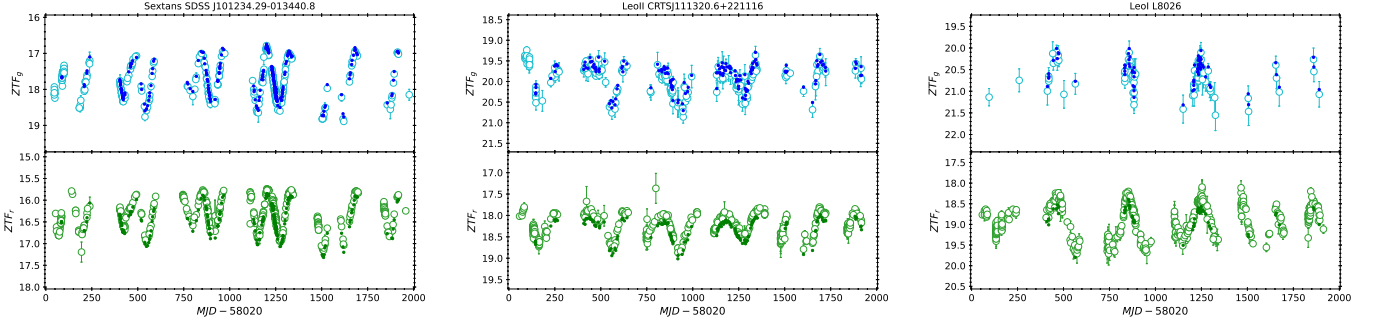


**Figure 8.** The  $gr$ -band ZTF light curves for the three short-period O-rich extragalactic Miras. The symbols are the same as in the right panels of Figure 2.

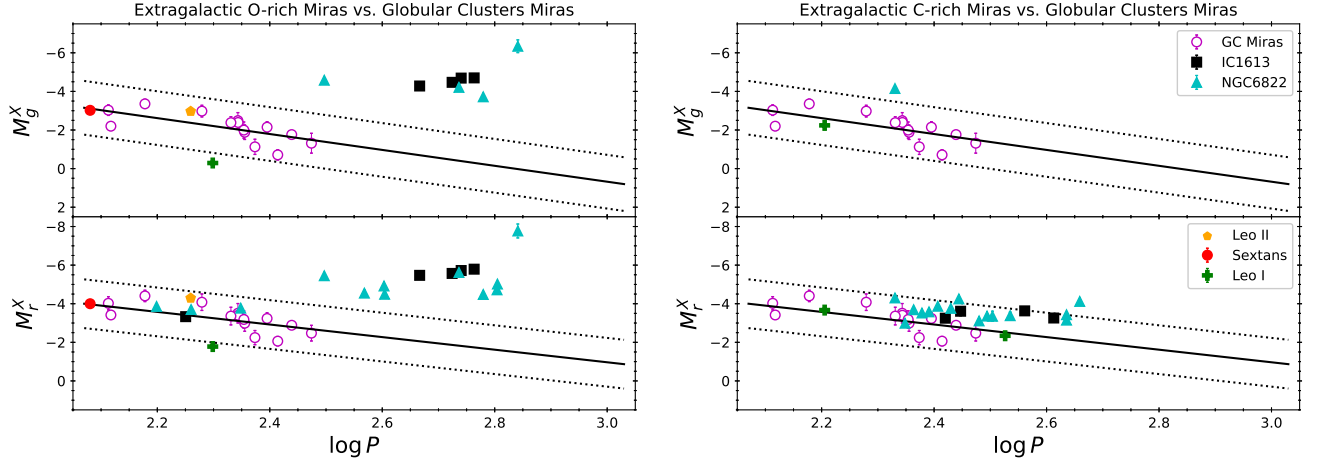


**Figure 9.** Comparison of the  $gr$ -band absolute magnitudes at maximum light between globular clusters Miras (open magenta circles) and extragalactic Miras (in various symbols). For extragalactic Miras, literature  $\mu$  (see text for details) were adopted to convert  $m_X$  to  $M_m^X$  (after corrected for extinction). The left and right panels are for the comparisons of O-rich Miras and C-rich Miras, respectively. The lines are the same as in Figure 6, but extrapolated to a longer period.

Figure 9 suggested the C-rich Miras seem to have a flat PL relation in the  $r$ -band.

## 6. DISCUSSION AND CONCLUSIONS

In this work, we derived the  $gr$ -band PL relations for the O-rich and short-period ( $< 300$  days) Miras in the globular clusters using the light-curve data collected from ZTF, as these globular clusters possess homogeneous distances compiled in Baumgardt & Vasiliev (2021). We focus on the maximum light when deriving the PL relations because Miras are known to exhibit a smaller PL dispersion at maximum light when compared to their mean-light counterparts. Furthermore, the  $(g - r)$  colors tend to be bluest at maximum light, implying the color-term corrections,  $C_m(g - r)$ , would be smaller when compared to other pulsation phases such as at mean light. Finally, due to the large-amplitude nature of Miras, it is possible that only the portions of the light curves around the maximum light could be detected for Miras located in distant galaxies. In this

scenario, measurements at maximum light can still be used to derive the distance moduli to the host galaxies, as we demonstrated in Section 5 for the Miras in NGC6822 and IC1613. Given that the limiting magnitude for ZTF is  $r \sim 20.6$  mag (Bellm et al. 2019a), the maximum light for a Mira with  $\log P = 2.3$ , based on equation (3), could be detected at a distance modulus of  $\mu \sim 23.9$  mag, which is within  $\pm 0.5$  mag from  $\mu_{\text{NGC6822}} = 23.4$  mag and  $\mu_{\text{IC1613}} = 24.3$  mag. For LSST, the single-epoch limiting magnitude in the  $r$ -band is  $\sim 24.7$  mag, implying a  $\log P = 2.3$  Mira could be detected up to  $\mu \sim 28$  mag at maximum light, corresponding to a distance of  $\sim 4$  Mpc.

In Figure 10, we presented the  $gr$ -band PL relations at maximum light for all of the Miras investigated in this work. In the  $r$ -band, which has more Miras than the  $g$ -band, both of the short-period O-rich and C-rich Miras seem to occupy the same region in the PL plane, suggesting our derived  $gr$ -band PL relations could also be used

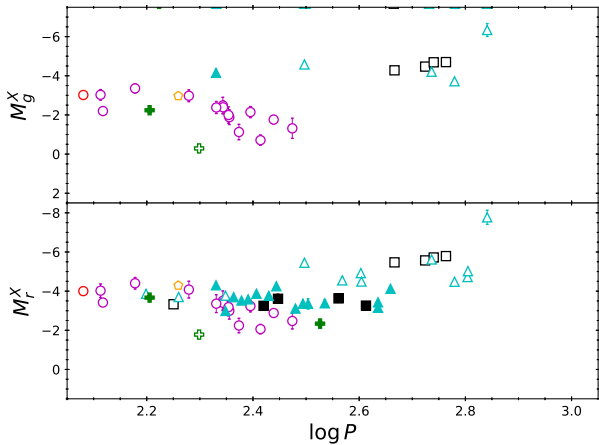


**Figure 10.** The PL relations at maximum lights for all of the Miras listed in Table 1 and 2. The symbols are same as in Figure 9. However, for a better visualization, open and filled symbols were used represent all of the O-rich and C-rich Miras, respectively.

for the short-period C-rich Miras (also, see the discussion in Section 5.3). However, as periods become longer, the long-period C-rich Miras appear to “connect” to the long-period HBB O-rich Miras. Altogether, the short- and long-period Miras formed a quadratic or segmented relation, hence the linear PL relations should only be applied to the short-period Miras. We suggest using short-period extragalactic Miras detected with LSST for distance measurements not only because they follow a linear relation, but also their periods will be better constraint from the 10 years observations.

#### ACKNOWLEDGMENTS

We are thankful for funding from the National Science and Technology Council (Taiwan) under the contracts 107-2119-M-008-014-MY2, 107-2119-M-008-012, 108-2628-M-007-005-RSP and 109-2112-M-008-014-MY3.

Based on observations obtained with the Samuel Oschin Telescope 48-inch Telescope at the Palomar

Observatory as part of the Zwicky Transient Facility project. ZTF is supported by the National Science Foundation under Grants No. AST-1440341 and AST-2034437 and a collaboration including current partners Caltech, IPAC, the Weizmann Institute of Science, the Oskar Klein Center at Stockholm University, the University of Maryland, Deutsches Elektronen-Synchrotron and Humboldt University, the TANGO Consortium of Taiwan, the University of Wisconsin at Milwaukee, Trinity College Dublin, Lawrence Livermore National Laboratories, IN2P3, University of Warwick, Ruhr University Bochum, Northwestern University and former partners the University of Washington, Los Alamos National Laboratories, and Lawrence Berkeley National Laboratories. Operations are conducted by COO, IPAC, and UW.

This publication makes use of data products from the Two Micron All Sky Survey, which is a joint project of the University of Massachusetts and the Infrared Processing and Analysis Center/California Institute of Technology, funded by the National Aeronautics and Space Administration and the National Science Foundation.

This research has made use of the SIMBAD database and the VizieR catalogue access tool, operated at CDS, Strasbourg, France. This research made use of Astropy,<sup>6</sup> a community-developed core Python package for Astronomy (Astropy Collaboration et al. 2013, 2018, 2022).

*Facility:* PO:1.2m

*Software:* astropy (Astropy Collaboration et al. 2013, 2018, 2022), dustmaps (Green 2018), gatspy (VanderPlas & Ivezić 2015), Matplotlib (Hunter 2007), NumPy (Harris et al. 2020), SciPy (Virtanen et al. 2020), statsmodels (Seabold & Perktold 2010).

#### REFERENCES

- Andriantsaralaza, M., Ramstedt, S., Vlemmings, W. H. T., et al. 2022, *A&A*, 667, A74
- Astropy Collaboration, Robitaille, T. P., Tollerud, E. J., et al. 2013, *A&A*, 558, A33
- Astropy Collaboration, Price-Whelan, A. M., Sipőcz, B. M., et al. 2018, *AJ*, 156, 123
- Astropy Collaboration, Price-Whelan, A. M., Lim, P. L., et al. 2022, *ApJ*, 935, 167
- Baumgardt, H. & Vasiliev, E. 2021, *MNRAS*, 505, 5957
- Bhardwaj, A., Kanbur, S., He, S., et al. 2019, *ApJ*, 884, 20
- Bedding, T. R. & Zijlstra, A. A. 1998, *ApJL*, 506, L47

<sup>6</sup> <http://www.astropy.org>

- Bellm, E. C., Kulkarni, S. R., Graham, M. J., et al. 2019a, *PASP*, 131, 018002
- Bellm, E. C., Kulkarni, S. R., Barlow, T., et al. 2019b, *PASP*, 131, 068003
- Chambers, K. C., Magnier, E. A., Metcalfe, N., et al. 2016, arXiv:1612.05560
- Clement, C. M., Muzzin, A., Dufton, Q., et al. 2001, *AJ*, 122, 2587
- Clement, C. M. 2017, *yCat*, V/150
- de Grijs, R. & Bono, G. 2014, *AJ*, 148, 17
- Dean, R. B. & Dixon, W. J. 1951, *Anal. Chem.*, 23, 636
- Dekany, R., Smith, R. M., Riddle, R., et al. 2020, *PASP*, 132, 038001
- Di Valentino, E., Mena, O., Pan, S., et al. 2021, *Classical and Quantum Gravity*, 38, 153001
- Drlica-Wagner, A., Bechtol, K., Mau, S., et al. 2020, *ApJ*, 893, 47
- Feast, M. W. 1984, *MNRAS*, 211, 51P
- Feast, M. W., Glass, I. S., Whitelock, P. A., et al. 1989, *MNRAS*, 241, 375
- Feast, M., Whitelock, P., & Menzies, J. 2002, *MNRAS*, 329, L7
- Feast, M. W., Whitelock, P. A., & Menzies, J. W. 2006, *MNRAS*, 369, 791
- Freedman, W. L. 2021, *ApJ*, 919, 16
- Glass, I. S. & Evans, T. L. 1981, *Nature*, 291, 303
- Glass, I. S. & Feast, M. W. 1982, *MNRAS*, 199, 245
- Glass, I. S. & Lloyd Evans, T. 2003, *MNRAS*, 343, 67
- Glass, I. S., Schultheis, M., Blommaert, J. A. D. L., et al. 2009, *MNRAS*, 395, L11
- Grady, J., Belokurov, V., & Evans, N. W. 2019, *MNRAS*, 483, 3022
- Graham, M. J., Kulkarni, S. R., Bellm, E. C., et al. 2019, *PASP*, 131, 078001
- Green, G. M. 2018, *The Journal of Open Source Software*, 3, 695
- Green, G. M., Schlafly, E., Zucker, C., et al. 2019, *ApJ*, 887, 93
- Groenewegen, M. A. T. & Whitelock, P. A. 1996, *MNRAS*, 281, 1347
- Hambleton, K. M., Bianco, F. B., Street, R., et al. 2022, arXiv:2208.04499
- Harris, C. R., Millman, K. J., van der Walt, S. J., et al. 2020, *Nature*, 585, 357
- Huang, C. D., Riess, A. G., Hoffmann, S. L., et al. 2018, *ApJ*, 857, 67
- Huang, C. D., Riess, A. G., Yuan, W., et al. 2020, *ApJ*, 889, 5
- Hughes, S. M. G. & Wood, P. R. 1990, *AJ*, 99, 784
- Hunter, J. D. 2007, *Computing in Science and Engineering*, 9, 90
- Ita, Y. & Matsunaga, N. 2011, *MNRAS*, 412, 2345
- Ita, Y., Menzies, J. W., Whitelock, P. A., et al. 2021, *MNRAS*, 500, 82
- Ivezić, Ž., Kahn, S. M., Tyson, J. A., et al. 2019, *ApJ*, 873, 111
- Iwanek, P., Soszyński, I., & Kozłowski, S. 2021a, *ApJ*, 919, 99
- Iwanek, P., Kozłowski, S., Gromadzki, M., et al. 2021b, *ApJS*, 257, 23
- Iwanek, P., Soszyński, I., Kozłowski, S., et al. 2022, *ApJS*, 260, 46
- Kanbur, S. M., Hendry, M. A., & Clarke, D. 1997, *MNRAS*, 289, 428
- Keeping, E. S. 1962, *Introduction to Statistical Inference* (Princeton, NJ: Van Nostrand-Reinhold)
- Macri, L. 2017, *EPJWC*, 152, 07001
- Magnier, E. A., Sweeney, W. E., Chambers, K. C., et al. 2020, *ApJS*, 251, 5
- Masci, F. J., Laher, R. R., Rusholme, B., et al. 2019, *PASP*, 131, 018003
- Matsunaga, N., Kawadu, T., Nishiyama, S., et al. 2009, *MNRAS*, 399, 1709
- Mattei, J. A. 1997, *JAAVSO*, 25, 57
- Menzies, J. W. & Whitelock, P. A. 1985, *MNRAS*, 212, 783
- Menzies, J., Feast, M., Tanabé, T., et al. 2002, *MNRAS*, 335, 923
- Menzies, J. W., Whitelock, P. A., Feast, M. W., et al. 2010, *MNRAS*, 406, 86
- Menzies, J. W., Whitelock, P. A., & Feast, M. W. 2015, *MNRAS*, 452, 910
- Ngeow, C.-C. 2022, *AJ*, 164, 45
- Origlia, L., Mucciarelli, A., Fiorentino, G., et al. 2019, *ApJ*, 871, 114
- Ou, J.-Y. & Ngeow, C.-C. 2022, *AJ*, 163, 192
- Ou, J.-Y., Ngeow, C.-C., Bhardwaj, A., et al. 2023, *AJ*, 165, 137
- Parada, J., Heyl, J., Richer, H., et al. 2023, *MNRAS*, 522, 195
- Reid, N., Glass, I. S., & Catchpole, R. M. 1988, *MNRAS*, 232, 53
- Rejkuba, M. 2004, *A&A*, 413, 903
- Riebel, D., Meixner, M., Fraser, O., et al. 2010, *ApJ*, 723, 1195
- Riess, A. G., Yuan, W., Macri, L. M., et al. 2022, *ApJL*, 934, L7
- Sakamoto, T., Matsunaga, N., Hasegawa, T., et al. 2012, *ApJL*, 761, L10
- Sanders, J. L. 2023, *MNRAS*, 523, 2369

- Seabold, S. & Perktold, J., Proceedings of the 9th Python in Science Conference, 2010
- Shah, P., Lemos, P., & Lahav, O. 2021, *A&A Rv*, 29, 9
- Skrutskie, M. F., Cutri, R. M., Stiening, R., et al. 2006, *AJ*, 131, 1163
- Sloan, G. C., Matsunaga, N., Matsuura, M., et al. 2010, *ApJ*, 719, 1274
- Soszyński, I., Udalski, A., Kubiak, M., et al. 2005, *Acta Astronomica*, 55, 331
- Sun, Y., Zhang, B., Reid, M. J., et al. 2022, *ApJ*, 931, 74
- Tabur, V., Bedding, T. R., Kiss, L. L., et al. 2010, *MNRAS*, 409, 777
- Templeton, M., Basu, S., & Demarque, P. 2002, *ApJ*, 576, 963
- van den Bergh, S. 1984, *Ap&SS*, 102, 295
- VanderPlas, J. T., & Ivezić, Ž. 2015, *ApJ*, 812, 18
- Verde, L., Treu, T., & Riess, A. G. 2019, *Nature Astronomy*, 3, 891
- Virtanen, P., Gommers, R., Oliphant, T. E., et al. 2020, *Nature Methods*, 17, 261
- Yuan, W., Macri, L. M., He, S., et al. 2017, *AJ*, 154, 149
- Yuan, W., Macri, L. M., Javadi, A., et al. 2018, *AJ*, 156, 112
- Whitelock, P. & Feast, M. 2000, *MNRAS*, 319, 759
- Whitelock, P. A., Feast, M. W., van Loon, J. T., et al. 2003, *MNRAS*, 342, 86
- Whitelock, P. A., Feast, M. W., & Van Leeuwen, F. 2008, *MNRAS*, 386, 313
- Whitelock, P. A. 2013, in *IAU Symp. 289, Advancing the Physics of Cosmic Distances*, ed. R. de Grijs (Cambridge: Cambridge Univ. Press), 209
- Whitelock, P. A., Menzies, J. W., Feast, M. W., et al. 2013, *MNRAS*, 428, 2216